Toxicol Res. (2021) 37:355–367
https://doi.org/10.1007/s43188-020-00072-z

eISSN 2234-2753
pISSN 1976-8257

ORIGINAL ARTICLE

Fimbristylis ovata extract and its ability to encounter AGEs-induced neurotoxicity in SH-SY5Y

Suphasarang Sirirattanakul[1] · Rachana Santiyanont[2]

Received: 8 December 2019 / Revised: 28 September 2020 / Accepted: 4 November 2020 / Published online: 25 January 2021

Abstract

Advanced glycation end products (AGEs) upon binding to its receptor (receptor for AGEs, RAGE) trigger several pathological processes involving oxidative stress and inflammatory pathway which play a pivotal role in various degenerative diseases including Alzheimer's disease. *Fimbristylis ovata* (*F. ovata*) has long been reported to be used as a traditional herbal medicine; nonetheless, very few studies have been reported. In this study, the protective effects of *F. ovata* extract on neurotoxicity of hippocampal neuronal cells (SH-SY5Y) was investigated. When compared to normal control, AGEs treatment significantly induced oxidative stress level and enhanced NF-κB translocation to nucleus in the neuronal cells ($p < 0.05$). The increase in NF-κB translocation leads to increase in transcription level of the target genes including RAGE and pro-inflammatory cytokines which include interleukin 1 beta (IL1B), tumor necrosis factor-alpha (TNFA) and interleukin 6 (IL6). Pre-treatment of SH-SY5Y with the extracts of *F. ovata* shows favorable results by significantly suppressing oxidative stress level ($p < 0.05$) as well transcriptional level of RAGE ($p < 0.05$) and pro-inflammatory cytokines ($p < 0.05$). Chemical analysis of *F. ovata* extracts using High Resolution Liquid Chromatograph Mass Spectrometer (HR-LCMS) and Gas Chromatograph with high resolution Mass Spectrometer (GC-HRMS) suggested some potential active phytochemical compounds. The results from this study may provide possible alternative treatment for prevention and/or therapy of neurodegenerative disorders by targeting the above-mentioned pathways. The role of the phytochemical active ingredient (s) in inhibiting the AGEs-triggered signaling inflammatory pathway should be investigated in future study.

✉ Rachana Santiyanont
rachana.s@chula.ac.th

[1] Graduate Program in Clinical Biochemistry and Molecular Medicine, Department of Clinical Chemistry, Faculty of Allied Health Sciences, Chulalongkorn University, Bangkok 10330, Thailand

[2] Department of Clinical Chemistry, Faculty of Allied Health Sciences, Chulalongkorn University, Bangkok 10330, Thailand

Graphic abstract

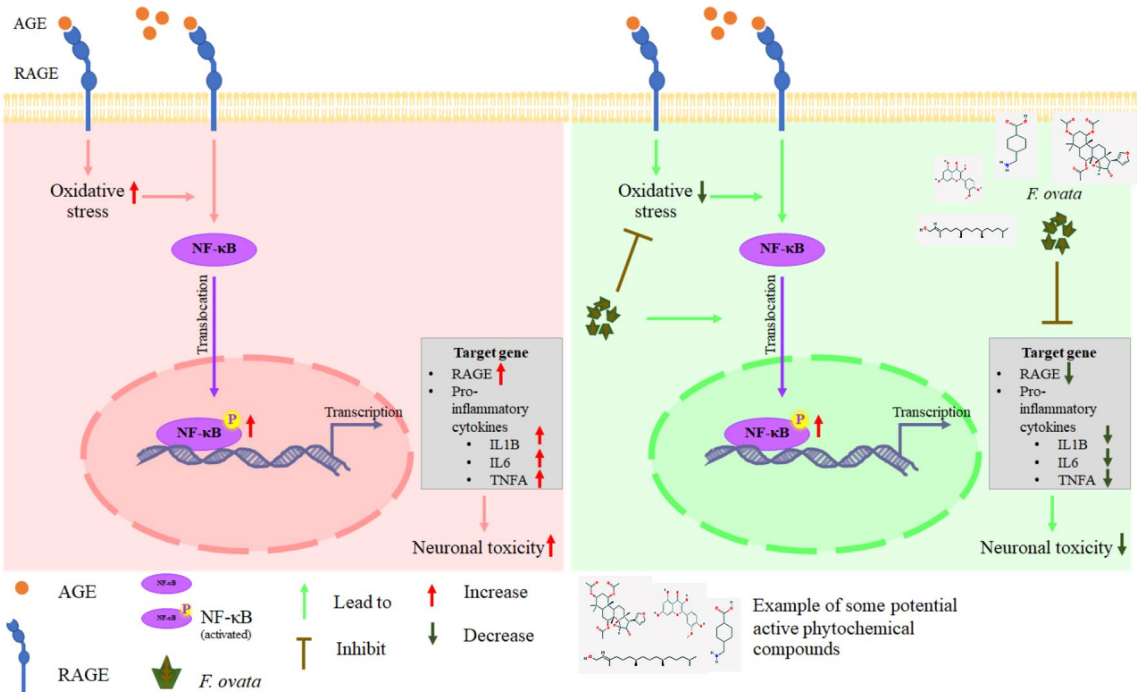

Keywords Neurotoxicity · Oxidative stress · Pro-inflammatory cytokines · *Fimbristylis ovata* · SH-SY5Y

Abbreviations

Aβ	Amyloid beta
AD	Alzheimer's disease
AGEs	Advanced glycation end products
DHE	Dihydroethidium
F. ovata	*Fimbristylis ovata* (Burm.f.) Kern
GC-HRMS	Gas chromatograph with high resolution mass spectrometer
HR-LCMS	High resolution liquid chromatograph mass spectrometer
IL1B	Interleukin 1 beta
IL6	Interleukin 6
MTS	3-(4,5-dimethylthiazol-2-yl)-5-(3-carboxymethoxyphenyl)-2-(4-sulfophenyl)-2H-tetrazolium) tetrazolium assay
NF-κB	Nuclear factor kappa light chain enhancer of activated B cells or nuclear factor kappa B
RAGE	Receptor for advanced glycation end products
ROS	Reactive oxygen species
SEM	Standard error of mean
SOD	Superoxide dismutase
TNFA	Tumor necrosis factor-alpha

Introduction

Brain is considered as a particular place vulnerable to oxidative injury due to its high oxygen utilization. The excessive free radicals and disturbance of antioxidant defense mechanism lead to neurotoxicity [1, 2]. Advanced glycation end-products (AGEs) may also employ their part in neurotoxicity through its capability of oxidative stress induction. Moreover, AGEs regulation involving intracellular reactive oxygen species (ROS) generation was found to enhance receptor of advanced glycation end-product (RAGE) expression, create positive feedback loops of AGEs signaling, and subsequently induce inflammatory reactions [3]. Previous studies demonstrated that AGEs levels were higher in the brain of Alzheimer's disease (AD) patients compared to the normal one and contributed to amyloid beta (Aβ) aggregation and plaque deposition. The presence of AGEs in plaque enriched fractions isolated from frontal cortex samples of AD brains contained 8.9 ± 1.4 AGEs units/mg of protein which was significantly about threefold higher than the corresponding preparations from healthy controls [4, 5]. Neurotoxicity is a well-recognized complication in various neurodegenerative disorders such as Alzheimer's disease and Parkinson's disease. Hence, the preventive and therapeutic strategy aiming to alleviate neurotoxicity's complication by suppressing

AGEs formation, AGEs/RAGE activation, and/or RAGE downstream pathway might be helpful for AD and other oxidative stress-induced diseases.

Fimbristylis ovata (Burm.f.) Kern (*F. ovata*) belongs to the genus *Fimbristylis* and family *Cyperaceae*. The plants in this family have long been reported to be used in wide range of medicinal and pharmacological applications according to the Ayurvedic system of medicine.

The usage activities including anti-oxidant property, wound healing activity, anti-pyretic and analgesic activity, anti-inflammatory activity, anti-histamine activity, anti-diarrheal activity, anti-hyperglycemic activity, anti-microbial activity, gastroprotective activity, hepatoprotective activity, cardioprotective and anti-hyperlipidemic, cytoprotective effect, hypotensive activity, anti-arthritic activity, and neuroprotective effect [6–8].

Extract from the plant in *Cyperaceae* family was revealed its neuroprotective potential in a rat model of cerebral ischemia–reperfusion which involved various pathophysiological mechanisms including excitotoxicity, inflammation and apoptosis. This post-ischemic status has significant forecasts toward complications that can lead to impaired cognition and memory. The study demonstrated that treatment with this extract increased the glutathione content in a dose dependent approach, increased superoxide dismutase (SOD) activity in all the brain structures, reduced the neurological deficits and reversed the anxiogenic behavior in rats [9]. Moreover, extract of *Cyperus rotundus*, one of *Cyperaceae* family, also revealed its neuroprotective potential against apoptotic event induced by SIN-1 (3-morpholinosydnonimine) [10]. Despite these vast variety studies of *Cyperaceae* family, only few studies on the effect of *F. ovata* were reported [11–13].

Previous studies of *F. ovata* extract which has been firstly reported in cultured monocytes and epithelial cells showed that this extract significantly decreases those inflammatory cytokines under oxidative stress induction [12]. Therefore, the role of *F. ovata* extract and its protective effects in SH-SY5Y, human neuroblastoma cell line, under neurotoxicity circumstance induced by AGEs were reported in this study for the first time. Potential active phytochemical compounds were identified by HR-LCMS and GC-HRMS.

Materials and methods

Chemicals and reagents

Advanced Glycation End Product-bovine serum albumin (AGEs-BSA), dimethyl sulfoxide (DMSO), and petroleum ether were purchased from Sigma-Aldrich (St. Louis, MO, USA). CellTiter 96® AQ_{ueous} One Solution Cell Proliferation Assay (MTS) was purchased from Promega (Madison, WI, USA). Fetal bovine serum (FBS), Penicillin/Streptomycin (10,000 U/mL) solution, Trypan Blue Solution, 0.4% solution, and Trypsin–EDTA (0.25%), and phenol red were purchased from Gibco (Waltham, MA, USA). Ethanol, methanol, isopropanol, Muse® Oxidative Stress Kit, and Amnis® NFkB Translocation Kit were purchased from Merck (Darmstadt, Germany). Trizol was purchased from Invitrogen (Carlsbad, CA, USA). Ham's F12 Nutrient Mixture and Minimum Essential Media (MEM) were purchased from Hyclone (Logan, UT, USA). AccuPower® CycleScript RT PreMix and AccuPower® 2X GreenStar Master Mix Solution were purchased from Bioneer (Daejeon, Korea).

Plant material and extract preparation

F. ovata, voucher No. 013431(BCU) *was* collected from a single source in Bangkok, Thailand. The plant was identified by Professor Kasin Suvatabhandhu Herbarium, Department of Botany, Faculty of Science, Chulalongkorn University, Thailand. The plant was dried and ground into fine powder, then extracted with petroleum ether and methanol 1:10 (w/v) by Soxhlet extraction. The extracts were filtered and evaporated. Crude extracts were dissolved in DMSO and stored as stock solution (100 mg/mL), at − 20 °C and protected from light until use.

Cell culture

Human neuroblastoma cell line, SH-SY5Y (a generous gift from Dr. Tewarit Sarachana, Faculty of Allied Health Sciences, Chulalongkorn University, Bangkok, Thailand), was used for all experiments. The cells were maintained in the Minimum Essential Medium: Nutrient Mixture F-12 (MEM/F12) (1:1) culture medium supplemented with 15% (v/v) FBS and 1% penicillin/streptomycin. The cell culture was incubated under a humidified 5% (v/v) CO_2-air environment at 37 °C. Prior to treatment with either AGEs-BSA with/without antioxidant compounds for the indicated times, the cells were plated and incubated overnight, dormant stage was conducted by a 24-h incubation with medium supplemented with 5% FBS.

Determination of cell viability

CellTiter 96® AQ_{ueous} One Solution Cell Proliferation was used for 3-(4,5-dimethylthiazol-2-yl)-5-(3-carboxymethoxyphenyl)-2-(4-sulfophenyl)-2H-tetrazolium) (MTS) tetrazolium assay cell viability assay. The method is based on the reduction capacity of mitochondrial enzymes in viable cells to generate a colored formazan product that is soluble in cell culture media. 20 µL of MTS solution was added to each well of the 96-well plate containing cell samples in 100 µL of culture medium. The plate

was incubated in the dark for 4 h at 37 °C in a humidified, 5% CO_2 atmosphere. Absorbance was measured at 490 nm using an EnSpire® Multimode Plate Reader (Perkin-Elmer, Waltham, MA, USA). All of viability tests were done after treatment with the designated substances (AGEs-BSA and *F. ovata* extract) for 24 h. Results are expressed as a percentage relative to untreated control.

Measurement of intracellular superoxide radicals

The Muse® Oxidative Stress Kit was used to measure intracellular superoxide radicals in cells undergoing oxidative stress. The method is based on dihydroethidium (DHE) dye, a fluorescence dye which can permeate the cell membrane. Once this dye reacts to superoxide radicals, the red fluorescence of DNA-binding fluorophore ethidium bromide will be formed. The product was then analyzed on the Muse™ Cell Analyzer according to the manufacturer's procedure. Briefly, SH-SY5Y cells were seeded in a density of 4×10^5 cell/mL in 12-well plates. After 24 h, the medium was changed to fresh 5% FBS medium. The cells were then treated with either AGEs-BSA with or without antioxidant compounds pre-treatment for the indicated times before proceeding to manufacture's protocol with slight modification. Pre-treatment with *F. ovata* and treatment with AGEs-BSA period were done for 3 h and an hour, respectively. Harvested cell samples were prepared at 1×10^6 cell in 100 µL of 1X assay buffer, 10 µL of prepared cell sample was used. 190 µL of Muse® oxidative stress intermediate solution was added to the prepared sample, then incubated for 30 min at 37 °C before being processed through Muse™ Cell Analyzer. 100 µM of H_2O_2 was used as a positive control.

Measurement of nuclear factor kappa light chain enhancer of activated B cells (NF-κB) translocation

Amnis® NFkB Translocation Kit was used to test the activation of NF-κB and its translocation to the nucleus. The quantitative measurement of NF-κB translocation from the cytoplasm to the nucleus was performed using the combination of flow cytometry and microscopic performance in one system to generate a quantitative result together with image data. This NF-κB translocation analysis is detected based on the correlation of the nuclear 7AAD (7-aminoactinomycin D) image to the anti-Hu NF-κB Alexa Fluor® 488 image. Briefly, SH-SY5Y cells were seeded in a density of 1×10^6 cell/mL in 6-well plates. After 24 h, the medium was changed to fresh 5% FBS medium. The cells were pretreated with either vehicle or *F. ovata* extracts for 3 h then incubated with 200 µg/mL of AGEs-BSA for 3 h before being trypsinized and proceeded to next step following manufacture's protocol with minor modification. The harvested cell samples were fixed with 1X fixation buffer for 10 min at room temperature, then washed with 1X assay buffer. Pellets were collected and incubated with anti-Hu NF-κB Alexa Fluor® 488/permeabilization buffer working solution for 30 min at room temperature. After that, washed and collected pellets. Resuspended the collected pellets in 0.25X fixation buffer, then incubated in 7AAD for 5 min. Next, the cell samples were analyzed by Amnis® Flowsight® and ImageStream® combined with the Nuclear Localization Wizard in the Amnis® IDEAS® software.

Ribonucleic acid (RNA) isolation and quantitative real-time polymerase chain reaction (real-time PCR)

Briefly, SH-SY5Y cells were seeded in a density of 1×10^6 cell/mL in 6-well plates. After 24 h, the medium was changed to fresh 5% FBS medium. The cells were pretreated with either vehicle or *F. ovata* extracts for 3 h then incubated with 200 µg/mL of AGEs-BSA for 24 h before total RNA isolation. Trizol reagent was used for total RNA extraction according to manufacturer's instructions with minimal adjustment. The amount of total RNA was assessed using a NanoDrop 1000 spectrophotometer (Thermo Fisher Scientific, Wilmington, DE, USA). 1 µg of total RNA as a template was reversely transcribed into complementary deoxyribonucleic acid (cDNA) using AccuPower® CycleScript RT PreMix reverse transcription system. The cDNA products were then amplified with each gene-specific primer pairs and quantitated using AccuPower® 2X GreenStar Master Mix Solution, a SYBR Green based Exicycler™ 96 Real-Time Quantitative Thermal Block system according to the protocol provided. The mRNA levels were then normalized with β-actin and calculated; the expression level was quantified as fold-change using the $\Delta\Delta C_t$ method ($2^{-\Delta\Delta C_t}$). The specific primer pairs using for all experiments were shown in Table 1. The thermal cycling conditions composed of an initial denaturation step at 95 °C for 10 min, followed by 35 cycles at 95 °C for 15 s and 62 °C for 30 s.

Table 1 Specific primer pairs for amplification of RAGE, IL1B, IL6, TNFA and β-actin

Gene	Primer pairs
RAGE	Forward: 5′-CAGCATCAGCATCATCGAACCA-3′ Reverse: 5′-CGCCTTTGCCACAAGATGACC-3′
IL1B	Forward: 5′-AGTACCTGAGCTCGCCAGTG-3′ Reverse: 5′-GGTCCTGGAAGGAGCACTTCAT-3′
IL6	Forward: 5′-CTTCTCCACAAGCGCCTTCG-3′ Reverse: 5′-TGTGGGGCGGCTACATCTTT-3′
TNFA	Forward: 5′-GCTGCACTTTGGAGTGATCGG-3′ Reverse: 5′-CTCAGCTTGAGGGTTTGCTACA-3′
β-actin	Forward: 5′-CTTCCTGGGCATGGAGTCCTGT-3′ Reverse: 5′-CTTTGCGGATGTCCACGTCAC-3′

Qualitative phytochemical screening

Phytochemical analysis of plant extracts was performed to identify the active components by High Resolution Liquid Chromatograph Mass Spectrometer (HR-LCMS) and Gas Chromatograph with high resolution Mass Spectrometer (GC-HRMS) using the service of Sophisticated Analytical Instrument Facility (SAIF), IIT-Bombay, India. The methanol extract of *F. ovata* was analyzed using HR-LCMS under the Agilent 6200 Series TOF and 6500 Series Q-TOF LC/MS system. HR-LCMS was performed in the electrospray ionization positive mode (+ESI mode). Putative compounds identification was assessed by comparing mass-to-charge ratio (m/z) values obtained from the experiment with SAIF library sources. Besides, the METLIN and the KNApSAcK databases as well as with the theoretical mass values from previously published data available were considered. A difference of less than 30 parts-per-million (ppm) was accepted.

The petroleum ether extract of *F. ovata* was analyzed using GC-HRMS. A Shimadzu GC-QP2010 with an autoinjector (AOC 20i) was used for this method. The separation was performed on a DB-5 column with 0.25 mm ID and 0.25 µm film thickness (Supelco) with an initial temperature set at 100 °C for 4 min. Followed by an increasing rate of 5 °C/min to 280 °C, which was held for 12 min at 250 °C was set for an injector temperature with 1 µL of an injection volume. The mass spectrometer was set to scan m/z range 50–600. The peaks were detected on the total ion chromatogram (TIC). NIST08.LIB9 and WILEY8.LIB10 library sources were used to identified mass spectra and the detected peaks. The instrument was operated in electron impact (EI +) positive ionization mode.

Statistical analysis

All experiments were performed at least in triplicate. Data were analyzed using SPSS statistical software. The data are shown as the mean ± SEM. Two-tailed Student's *t* test was used to determine the statistical significance of differences between two groups. Differences between the values were considered significant at *p*-values less than 0.05.

Results

Cell viability of human neuroblastoma cells, SH-SY5Y, which were exposed to AGEs or *F. ovata* extracts

To determine cell viability upon AGEs-BSA or *F. ovata* extracts treatment, MTS tetrazolium assay was used. SH-SY5Y cells were exposed to AGEs-BSA at various concentrations ranging from 100 to 800 µg/mL for 24 h. Result showed that cell viability was greater than 80% in all treatments (Fig. 1). Result from 24 h' exposure of SH-SY5Y to various concentrations of *F. ovata* extracts (either petroleum ether or methanol extract) ranging from 3.125 to 100 µg/mL demonstrated that the cells viability was greater than 80% in all treatments (Fig. 2).

F. ovata protects SH-SY5Y against AGEs-induced oxidative stress

In this part, the cellular populations undergoing oxidative stress with either H_2O_2 (positive control) or AGEs-BSA (200, 400, and 600 µg/mL) were measured quantitatively by flow cytometer based on a relative detection of superoxide

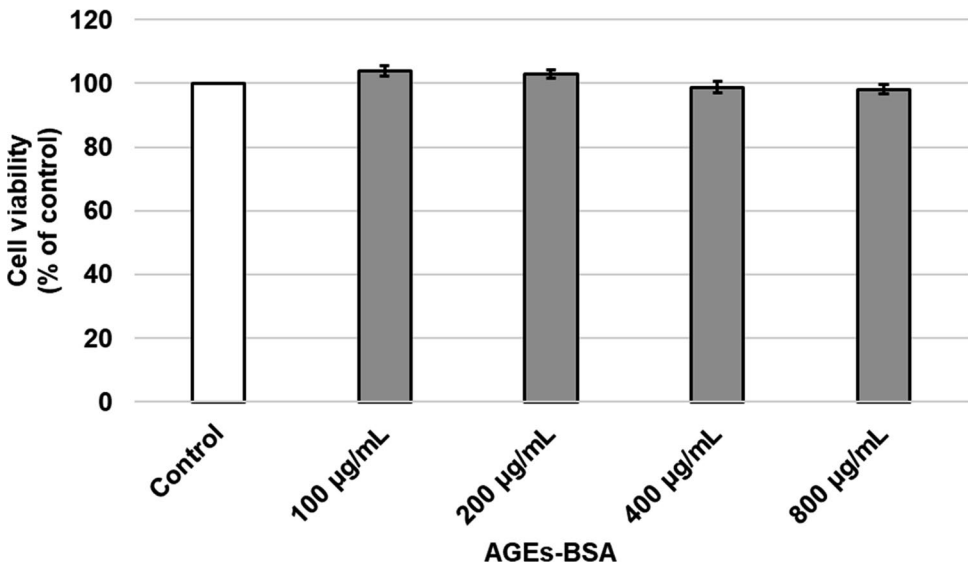

Fig. 1 The effect of AGEs treatment on SH-SY5Y cells viability. SH-SY5Y cells were incubated with AGEs-BSA at various concentrations ranging from 100 to 800 µg/mL for 24 h to test on AGEs-BSA toxicity by MTS assay. The differences in the mean values among the treatment groups are reported as clustered columns with their standard error of mean (SEM) (mean ± SEM). All experiments were done in at least three independent experiments

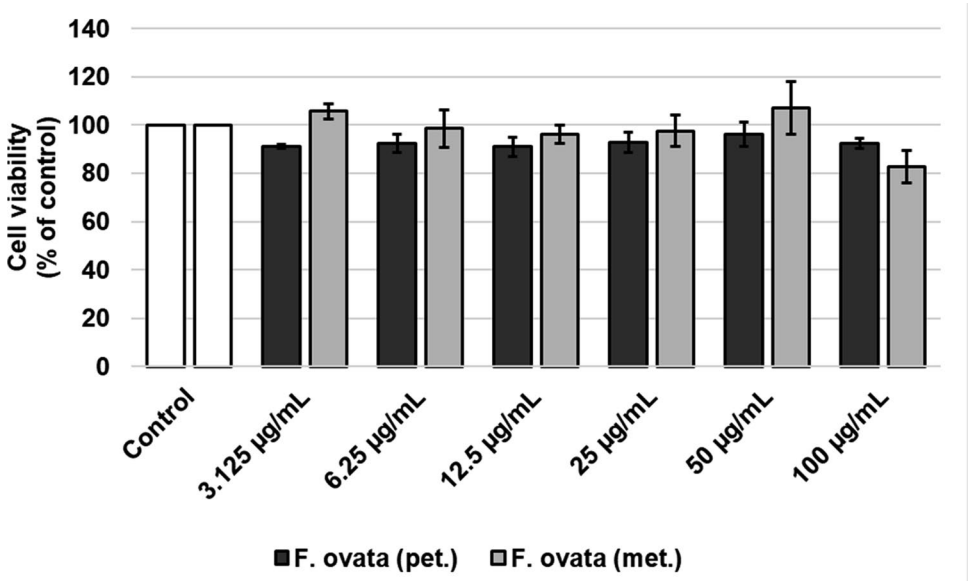

Fig. 2 The effects of *Fimbristylis ovata* extracts on cell viability in human neuroblastoma SH-SY5Y. The cells were exposed to either 0.1% DMSO vehicle control or extraction of *F. ovata*; *F. ovata* (pet.; petroleum ether) or *F. ovata* (met.; methanol) extracts ranging from 3.125 to 100 µg/mL for 24 h, then were determined by MTS assay. The differences in the mean values among the treatment groups are reported as clustered columns with their standard error of mean (SEM) (mean ± SEM). All experiments were done in at least three independent experiments

radical production in cellular population using DHE-based assay (Fig. 3). The results show that AGEs significantly increase intracellular superoxide radical production at 200, 400, and 600 µg/mL in a dose-dependent manner ($p < 0.05$). We hypothesized that *F. ovata* might exert its role as a protective agent against oxidative stress condition induced by AGEs-BSA. SH-SY5Y cells were pretreated with either *F. ovata* petroleum ether extract, *F. ovata* (pet.) or *F. ovata* methanol extract, *F. ovata* (met.) at 100 µg/mL for 3 h. The cells were then incubated with 200 µg/mL AGEs-BSA for an hour. The results showed that *F. ovata* obtained from both petroleum ether and methanol fractions significantly decreased oxidative stress induced by AGEs-BSA ($p < 0.05$) (Fig. 4). This result suggests that *F. ovata* protects against AGEs-induced cytotoxicity as being demonstrated by decrease in intracellular superoxide radical production.

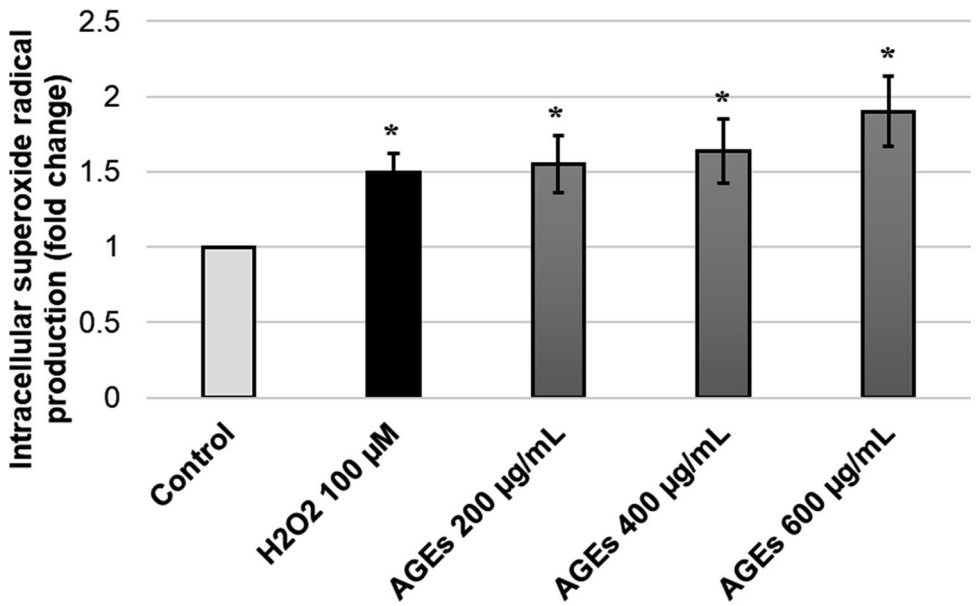

Fig. 3 Effect of AGEs at various concentrations on intracellular superoxide radical levels. The relative percentage of cells exhibiting intracellular superoxide radical was determined after SH-SY5Y cells undergoing AGEs-BSA treatment for an hour. H_2O_2 was used as a positive control. Flow cytometry analyzer was used based on dihydroethidium (DHE) reagent detection. The differences in the mean values among the treatment groups are reported as clustered columns with their standard error of mean (SEM) (mean ± SEM). All experiments were done in at least three independent experiments; statistical difference will be considered when $p < 0.05$. When compared to control, H_2O_2 and AGEs-treated cell at various concentrations were given $p = 0.0177$*, 0.0440*, 0.0408*, and 0.0174*, respectively

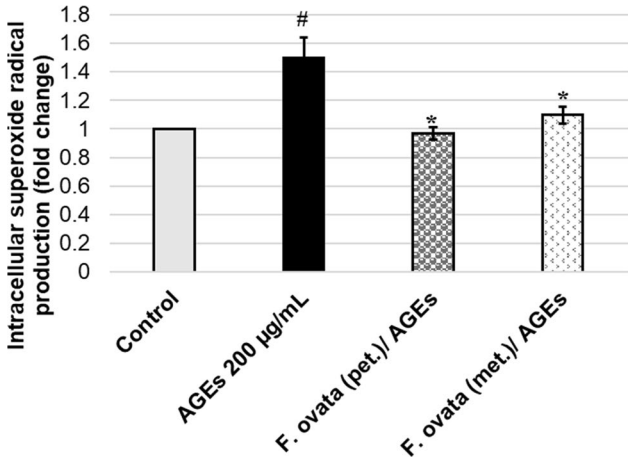

Fig. 4 Effect of *F. ovata* extracts on protection of AGEs-treated neuronal cells (SH-SY5Y). Using the cultured SH-SY5Y cells, vehicle control containing 0.1% DMSO or 100 µg/mL of either *F. ovata* (pet.; petroleum ether) or *F. ovata* (met.; methanol) extract was added and incubated as a pre-treatment, followed by addition and incubation with 200 µg/mL AGEs-BSA. The relative percentage of cells exhibiting intracellular superoxide radical was evaluated. The differences in the mean values among the treatment groups are reported as clustered columns with their standard error of mean (SEM) (mean ± SEM). All experiments were done in at least three independent experiments; statistical difference when $^{\#}p < 0.05$ vs 0.1% DMSO vehicle control; $^{*}p < 0.05$ vs AGEs-induced. When compare to vehicle control, AGEs-induced cells gave $p = 0.0138^{\#}$. When compare *F. ovata* extracts (pet. and met.) pre-treated cells with AGEs-induced cells, the results showed $p = 0.0127^{*}$, and 0.0421^{*}, respectively

NF-κB translocation determination in response to AGEs treatment on SH-SY5Y cells

The activation of NF-κB and its translocation to the nucleus plays a crucial role in regulating many key processes in mammalian cells which led us to studying cellular function, signal transduction pathways, disease mechanisms and drug discovery. NF-κB p50/p65 heterodimer, the most abundant form, is kept in inactive state by its inhibitor (inhibitor of NF-κB; IκB). Once the IκB is phosphorylated, NF-κB complex becomes activated and translocated into nucleus which can be detected by the Anti-Hu NF-κB Alexa Fluor® 488 antibody in correlation to the nuclear 7AAD dye (Fig. 5). We found that SH-SY5Y cells exposed to 200 µg/mL AGEs-BSA for 3 h significantly increased NF-κB translocation to nucleus compared to the vehicle control. Unexpectedly, pretreatment with either 100 µg/mL of *F. ovata* petroleum ether extracts (pet.) or *F. ovata* methanol extracts (met.) for 3 h prior to AGEs exposure also showed a significant enhancement of translocated NF-κB in the nucleus compared to AGEs treatment alone ($p < 0.05$) (Fig. 6).

F. ovata extract suppress mRNA expression of RAGE and pro-inflammatory cytokines in AGEs-treated SH-SY5Y

In this part, SH-SY5Y cells were pretreated with either vehicle control containing 0.1% DMSO or *F. ovata* extracts for 3 h, then treated with 200 µg/mL AGEs-BSA for 24 h. The result showed that exposure to 200 µg/mL of AGEs-BSA for 24 h significantly increase mRNA expression levels of RAGE, interleukin 1 beta (IL1B), interleukin 6 (IL6), and tumor necrosis factor alpha (TNFA) ($p < 0.05$). When the cells were pre-treated with either petroleum ether or methanol extracts of *F. ovata*, RAGE, IL6, and TNFA expression levels were significantly decreased ($p < 0.05$). IL1B was significantly reduced by pretreatment with methanol extracts ($p < 0.05$), as well with petroleum ether extract but not significantly (Fig. 7). Hence, these results demonstrate that *F. ovata* extract provides a suppressing action against RAGE expression and inflammatory response induced by AGEs treatment.

Phytochemical constituents of *F. ovata*

HR-LCMS analysis of methanol extract of *F. ovata* and GC-HRMS analysis of petroleum ether extract of *F. ovata* were carried out in order to identify the active phytochemical constituents which were mainly focused on the compounds responsible for neuroprotective and/or anti-aging event. Based on m/z values in the positive mode obtained from total ion chromatogram (TIC), each spectrum peak was identified and compared to databases and literatures. According to the result obtained from HR-LCMS analysis of methanol extract of *F. ovata*, we reported 9 potential peaks indicating phytochemical constituents in charge of neuroprotective and/or anti-aging properties (Fig. 8). The identified compounds are 2-amino-3-methyl-1-butanol, tranexamic acid, neuraminic acid, 4-hydroxystyrene, swietenine, isorhamnetin, crocetin, khayanthone, and trandolapril glucuronide (Table 2). Thirteen isolated peaks were found in GC-HRMS analysis of petroleum ether extract of *F. ovata*. We reported five candidate compounds having the possible role as a neuroprotective and/or anti-aging substance (Fig. 9). The identified compounds are 2-pentadecanone, 6,10,14-trimethyl-, n-hexadecanoic acid, phytol, 9,12,15-octadecatrienoic acid, [Z,Z,Z]-, and octadecanoic acid (Table 3).

Discussion

The receptor for advanced glycation end products (RAGE or AGER) is a major receptor for AGEs, its interaction with AGEs activates several signaling pathways in different cell types including p38 mitogen-activated protein

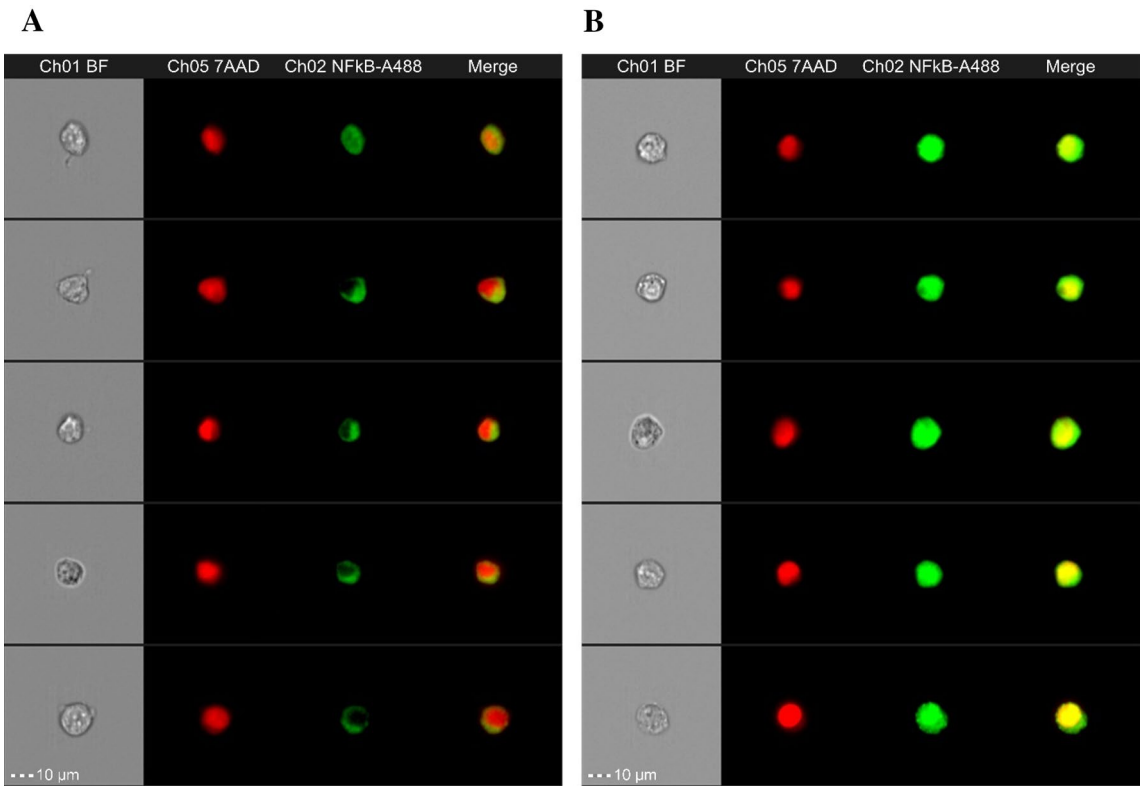

Fig. 5 Translocation of NF-κB in AGEs-treated SH-SY5Y. The ×40 composite images of the anti-Hu NF-κB Alexa Fluor® 488 (green) and the nuclear 7AAD (red) is delivered from Amnis® Flowsight® and ImageStream® combined with the Nuclear Localization Wizard in the Amnis® IDEAS® software. Following data acquisition, the pixel intensity correlation between the anti-Hu NF-κB Alexa Fluor® 488 (green) and the nuclear image 7AAD (red) was calculated as similarity score for every cell. Cells with low similarity scores indicate a dissimilar between the image (un-translocated cell; control) (**a**), while cells with high similarity scores indicate a positive correlation between the image (translocated cell; AGEs-treated SH-SY5Y) (**b**)

kinase (MAPK), NF-κB, cell division control protein 42/Ras-related C3 botulinum toxin substrate (CDC42/Rac), stress-activated protein kinase/c-Jun N-terminal kinases (SAPK/JNK), and Janus kinase/signal transducer and activator of transcription (JAK/STAT) pathways [14]. Increased free radicals and disturbance of antioxidant defense mechanism in brain lead to neurotoxicity. Results from this study demonstrates that oxidative stress level was induced by AGEs treatment. Translocated NF-κB was also increased upon exposure to AGEs, this perhaps due to the elevation of oxidative stress level or directly by RAGE activation. The major feature of this event is NF-κB and SP1 elements which are located on RAGE gene promoter [15]. These transcription elements are responding to pro-inflammatory cellular signaling by increased RAGE expression. Hence, a positive feedback mechanism driven by cell-surface RAGE/ligand interaction is set up. Moreover, the increase in NF-κB translocation leads to the additional transcription level of the target genes including RAGE and pro-inflammatory cytokines (IL1B, IL6, and TNFA). The results revealed that oxidative stress level and transcriptional level of RAGE and pro-inflammatory cytokines which were induced by AGEs were suppressed by *F. ovata* extract treatment.

The activation of NF-κB and its translocation from the cytoplasm to the nucleus regulates many cellular processes including proliferation, differentiation, inflammation, apoptosis, and survival. Moreover, this transcription factor involves in brain-specific processes such as the synaptic signaling that underlies learning and memory, these functions have been reviewed previously [16, 17]. NF-κB is activated by a wide variety of stimuli, and its dysregulation is often implicated in inflammation. An increase in cytokines production such as IL1B, TNFA, IL6 is common mediators and associated with neuronal injury that altered central nervous system (CNS) function during inflammatory states in both acute and chronic age-related neurodegenerative diseases such as colitis, multiple sclerosis, acute liver failure, amyotrophic lateral sclerosis, and Alzheimer's disease [18, 19]. Our study showed that translocated NF-κB and transcriptional pro-inflammatory cytokines were increased upon exposure to AGEs. The treatment with *F. ovata* significantly reduced pro-inflammatory cytokines level but did not

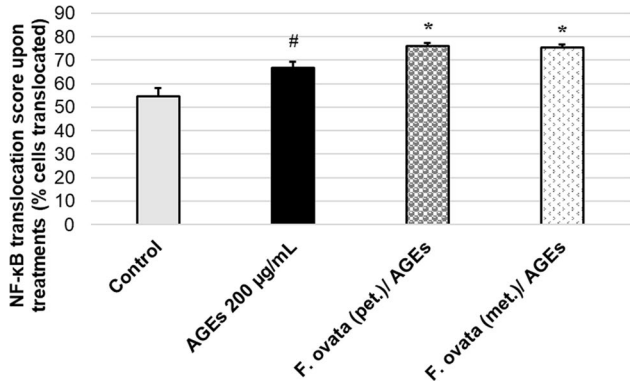

Fig. 6 Effect of *F. ovata* extracts on NF-κB translocation under AGEs treatment condition. SH-SY5Y cells were pretreated with either 0.1% DMSO (as vehicle control) or *F. ovata* (pet.; petroleum ether) or *F. ovata* (met.; methanol) extracts for 3 h, then treated with 200 µg/mL AGEs-BSA for 3 h. *F. ovata* extracts from both petroleum ether and methanol fractions at 100 µg/mL can significantly increase NF-κB translocation. The similarity scores (translocated cell score) were created using the Nuclear Localization Wizard in the Amnis® IDEAS® software showing the similarity feature which calculates a pixel by pixel of the correlation between the anti-Hu NF-κB Alexa Fluor® 488 and the nuclear 7AAD. The differences in the mean values among the treatment groups are reported as clustered columns with their standard error of mean (SEM) (mean ± SEM). All experiments were done in at least three independent experiments; statistical difference when $^{\#}p < 0.05$ vs 0.1% DMSO control; $^{*}p < 0.05$ vs AGEs-induced. When compare to vehicle control, AGEs-induced cells gave $p = 0.0229^{\#}$. When compare *F. ovata* extracts (pet. and met.) pre-treated cells with AGEs-induced cells, the results showed $p = 0.0311^{*}$, and 0.0414^{*}, respectively

suppress NF-κB translocation. This perhaps due to another involving element which leads to the inhibition of NF-κB transcriptional activity. For example, p50/p50 homodimers which compete for κB sites with p50/p65 resulting in gene activation inhibition, IκB-α, inhibitors of κB-α, which inhibit NF-κB transcriptional activity by interacts with p50/p65 in the nucleus, CREB-binding protein (CBT) which significantly decreased the efficiency of NF-κB transcription but not NF-κB nuclear translocation, by disruption of its interaction with NF-κB encountered with the elevation of intracellular cyclic AMP (cAMP) and activation of protein kinase A (PKA) [20, 21].

In this study, phytochemical constituents' analysis of *F. ovata* was determined by HR-LCMS for the methanol extract and GC-HRMS for the petroleum ether extract. Various interesting compounds were identified. For example, 2-Amino-3-methyl-1-butanol or Valinol is part of numerous pharmaceuticals including drugs for inhibition of HIV (as integrase inhibitors), treatment of hepatitis C virus (as HCV inhibitor), treatment of diabetes and obesity (as PPRAG modulators) as well as non-opioid analgesic agents [22]. Tranexamic acid, a known antifibrinolytic agent, has been previously demonstrated to exert its role in anti-inflammatory properties by suppressing IL6 and TNFA levels [23, 24]. Neuraminic acid is a sialic acid which abundantly found in mammalian brain but decline gradually over time. Its crucial roles have been identified in many neural structures and functions such as neuronal survival, neural growth and brain development, synaptic plasticity and memory [25, 26]. Swietenine is a triterpenoid which has been reported for its antifeedant activity, and antidiabetic activity (by increasing the translocation of Glucose transporter type 4 (GLUT4) to the plasma membrane) [27, 28]. The relationship between type 2 diabetes mellitus (DM) and neurodegenerative disorders such as Alzheimer's disease has been reported in several types of studies. The decrease in GLUT4 translocation has been described as a one of related causative events to the alteration in both AD and DM. Therefore, Swietenine is possibly a curative agent for these disease via GLUT4 signaling [29, 30]. Isorhamnetin, a methylated metabolite of quercetin, has been reported to take a role in anti-inflammatory (by decreasing TNFA, IL1B, and IL6 concentration), antioxidant, learning and memory [31–33]. Crocetin is a diterpenoid and a natural carotenoid. Its properties have been possessed in cognitive function improvement, anti-inflammation (by increasing TNFA, IL1B, IL8, and IL6, while increasing IL10), anti-apoptosis, and neuroprotective agent [34–36]. Phytol is a diterpenoid which abundantly found as a constituent of chlorophyll and commonly used as a precursor for the manufacture of synthetic forms of vitamin E and vitamin K [37, 38]. 9,12,15-Octadecatrienoic acid, [Z,Z,Z]- or linolenic acid, an essential fatty acid belonged to the omega-3 fatty acids group. It possessed properties in brain development and function. A dietary supplement of this fatty acid gave favorable result in neuropsychiatric disorders, particularly depression, as well as in dementia, notably Alzheimer's disease prevention [39]. Octadecanoic acid or stearic acid is a saturated long-chain fatty acid with an 18-carbon backbone which has influence in neurogenesis. Thus, this agent was suggested to be used to control neurodevelopmental syndromes, cognitive decline during aging, and various psychiatric disorders [40].

In conclusion, AGEs which enhance oxidative stress level in neuronal cells may contribute to neurodegenerative disease such as AD by intervening ROS balance and pro-inflammatory cytokine over-production. In particular, oxidative damage is one of the earlier causative event occurring in age-related dementia [41, 42]. As well, excessive inflammatory cytokine response plays a crucial part in the disease complication which is unfavorable for the diseases [43]. The present results give an insight into the possible new agent aiming for the strategy of reducing oxidative damage and inflammation in AD.

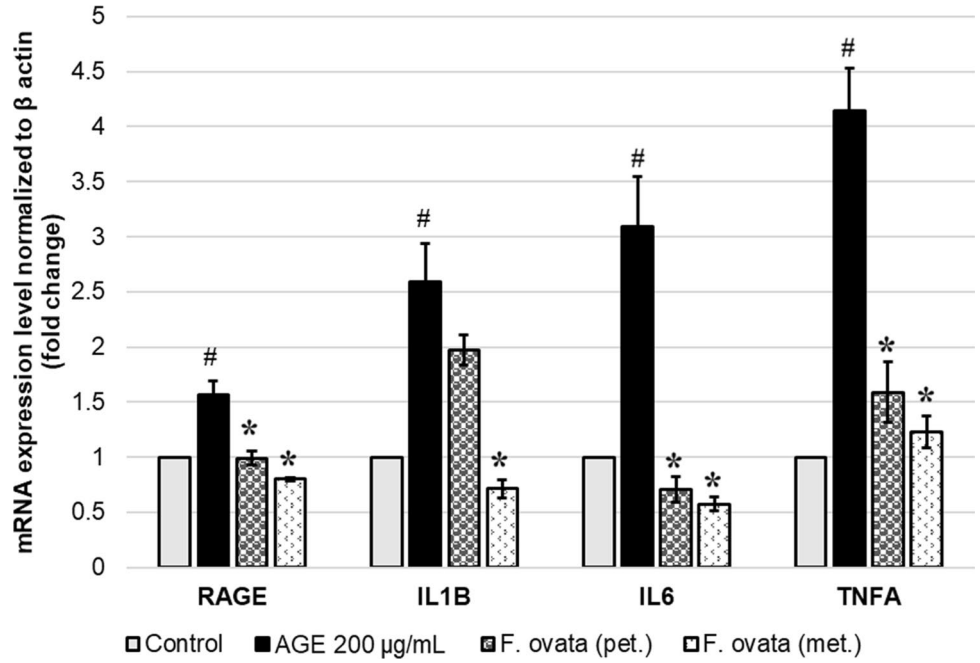

Fig. 7 Effect of *F. ovata* extracts on mRNA expression of RAGE and pro-inflammatory cytokines induced by AGEs. Normalized expression ratio of each gene against housekeeping genes (β actin) is shown on the primary vertical axis comparing SH-SY5Y cells which were pretreated with either 0.1% DMSO vehicle control or *F. ovata* (either pet.; petroleum ether or met.; methanol) extracts for 3 h, then treated with 200 µg/mL AGEs-BSA for 24 h. The differences in the mean values among the treatment groups are reported as clustered columns with their standard error of mean (SEM) (mean ± SEM). All experiments were done in at least three independent experiments; statistical difference when $^{\#}p < 0.05$ vs 0.1% DMSO control; $^{*}p < 0.05$ vs AGEs-induced. When compare to vehicle control, AGEs-induced cells gave $p = 0.0044^{\#}$, $0.0039^{\#}$, $0.0036^{\#}$, and $0.0002^{\#}$ for RAGE, IL1B, IL6, and TNFA, respectively. When compare *F. ovata* extracts (pet. and met.) pre-treated cells with AGEs-induced cells, for RAGE; $p = 0.0067$*, and 0.0010*, for IL1B; $p = 0.1529$, and 0.0020*, for IL6; $p = 0.0023$*, and 0.0015*, for TNFA; $p = 0.0017$*, and 0.0004*

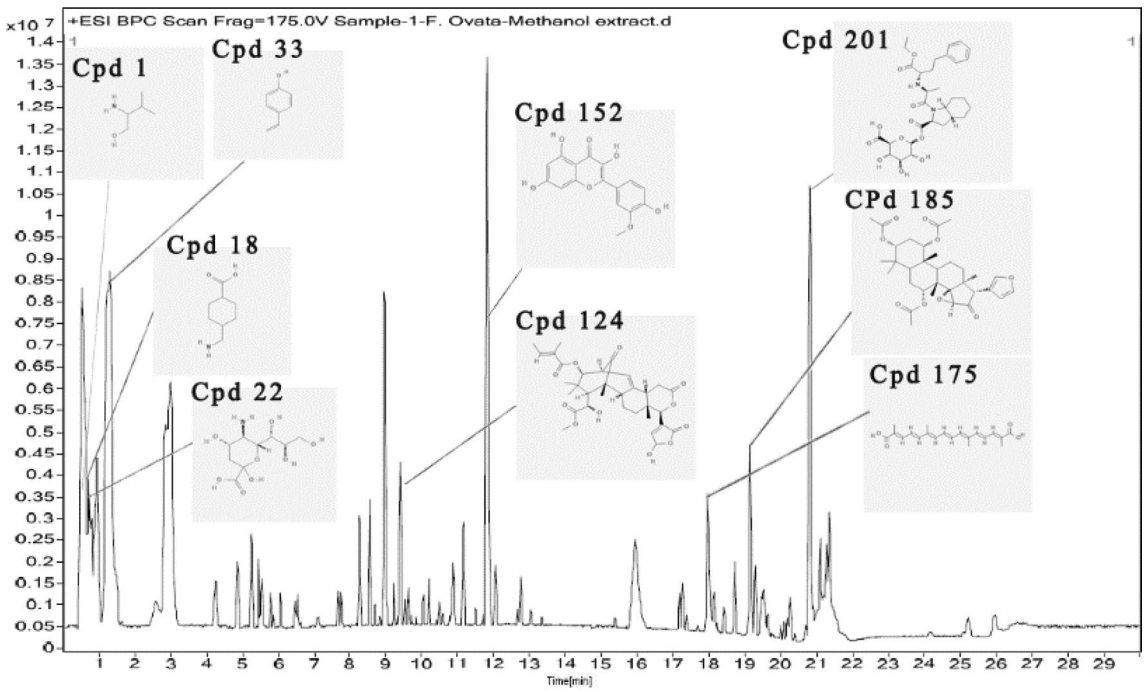

Fig. 8 HR-LCMS chromatogram analysis of *F. ovata* methanol extract. An analysis of *F. ovata* methanol extract by HR-LCMS is presented as chromatogram of mass spectrum and retention time of each fragment. The structures of compound 1 (Cpd 1: 2-amino-3-methyl-1-butanol), 18 (Cpd 18: tranexamic acid), 22 (Cpd 22: neuraminic acid), 33 (Cpd 33: 4-hydroxystyrene), 124 (Cpd 124: swietenine), 152 (Cpd 152: isorhamnetin), 175 (Cpd 175: crocetin), 185 (Cpd 185: khayanthone), and 201 (Cpd 201: trandolapril glucuronide) are displayed

Table 2 Proposed phytochemical constituents in methanol extract of *F. ovata*

No.	Compound label	RT (min)	Mass	DB diff (ppm)
1	Cpd 1: 2-amino-3-methyl-1-butanol	0.499	103.10	6.97
2	Cpd 18: tranexamic acid	0.717	157.11	6.04
3	Cpd 22: neuraminic acid	0.747	267.09	2.91
4	Cpd 33: 4-hydroxystyrene	1.284	120.06	6.52
5	Cpd 124: swietenine	9.405	568.27	−6.66
6	Cpd 152: isorhamnetin	11.822	316.06	5.39
7	Cpd 175: crocetin	17.974	328.17	5.25
8	Cpd 185: khayanthone	19.151	570.28	−0.87
9	Cpd 201: trandolapril glucuronide	20.816	606.28	−4.00

Putative compounds identification was assessed by comparing m/z values obtained from the experiment with those from the databases. Database difference (DB diff) of less than 30 parts-per-million (ppm) was accepted

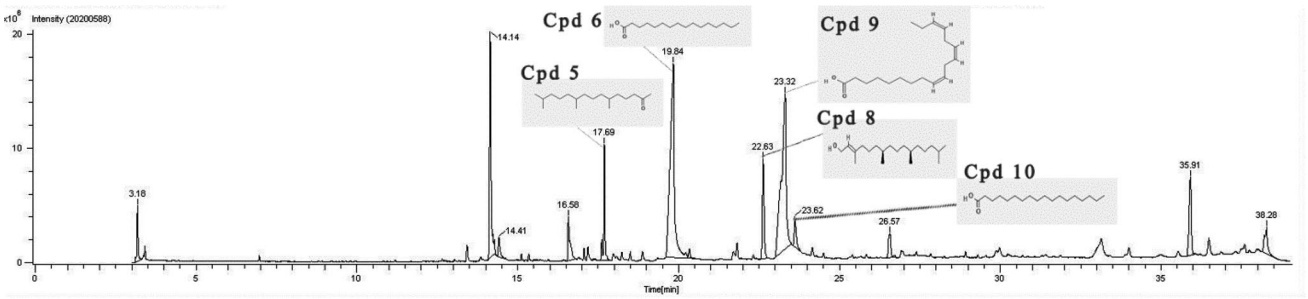

Fig. 9 GC-HRMS chromatogram analysis of *F. ovata* petroleum ether extract. An analysis of *F. ovata* petroleum ether extract by GC-HRMS is presented as chromatogram of mass spectrum and retention time of each fragment. The structures of compound 5 (Cpd 5: 2-pentadecanone, 6,10,14-trimethyl-), 6 (Cpd 6: n-hexadecanoic acid), 8 (Cpd 8: phytol), 9 (Cpd 9: 9,12,15-octadecatrienoic acid, [Z,Z,Z]-), and 10 (Cpd 10: octadecanoic acid) are displayed

Table 3 Proposed phytochemical constituents in petroleum ether of *F. ovata*

No.	Compound label	RT (min)	Mass	%Match
1	Cpd 5: 2-pentadecanone, 6,10,14-trimethyl-	17.69	268	92.7
2	Cpd 6: n-hexadecanoic acid	19.84	256	82.3
3	Cpd 8: phytol	22.63	296	77.8
4	Cpd 9: 9,12,15-octadecatrienoic acid, [Z,Z,Z]-	23.32	278	43.5
5	Cpd 10: octadecanoic acid	23.62	284	44.6

The peaks were detected on the total ion chromatogram (TIC). NIST08.LIB9 and WILEY8.LIB10 library sources were used to identify mass spectra and the detected peaks

Acknowledgements We thank Dr. Suporn Sukjamnong for technical support in plant material and extract preparation. This work was granted by Chulalongkorn University Graduate Scholarship to Commemorate the 72nd Anniversary of His Majesty King BhumibolAdulyadej, The 90th Anniversary of Chulalongkorn University Fund (Ratchadaphiseksomphot Endowment Fund), and Asia Research Center, Chulalongkorn University (ARC) (contract no. 005/2560).

Compliance with ethical standards

Conflict of interest All authors declare no conflict of interest to disclose.

References

1. Sattler R, Tymianski M (2001) Molecular mechanisms of glutamate receptor-mediated excitotoxic neuronal cell death. Mol Neurobiol 24:107–129. https://doi.org/10.1385/MN:24:1-3:107
2. Hastings TG (2009) The role of dopamine oxidation in mitochondrial dysfunction: implications for Parkinson's disease. J Bioenerg Biomembr 41:469–472. https://doi.org/10.1007/s10863-009-9257-z
3. Yamagishi S (2011) Role of advanced glycation end products (AGEs) and receptor for AGEs (RAGE) in vascular damage in diabetes. Exp Gerontol 46:217–224. https://doi.org/10.1016/j.exger.2010.11.007
4. Vitek MP, Bhattacharya K, Glendening JM, Stopa E, Vlassara H, Bucala R, Manogue K, Cerami A (1994) Advanced glycation end products contribute to amyloidosis in Alzheimer disease. Proc Natl Acad Sci USA 91:4766–4770. https://doi.org/10.1073/pnas.91.11.4766
5. Munch G, Mayer S, Michaelis J, Hipkiss AR, Riederer P, Muller R, Neumann A, Schinzel R, Cunningham AM (1997) Influence of advanced glycation end-products and AGE-inhibitors on nucleation-dependent polymerization of beta-amyloid peptide. Biochem Biophys Acta 1360:17–29. https://doi.org/10.1016/S0925-4439(96)00062-2
6. Kamala A, Middha SK, Karigar CS (2018) Plants in traditional medicine with special reference to *Cyperus rotundus* L.: a review. 3 Biotech 8:309. https://doi.org/10.1007/s13205-018-1328-6
7. Arraki K, Totoson P, Decendit A, Badoc A, Zedet A, Jolibois J, Pudlo M, Demougeot C, Girard-Thernier C (2017) Cyperaceae species are potential sources of natural mammalian arginase inhibitors with positive effects on vascular function. J Nat Prod 80:2432–2438. https://doi.org/10.1021/acs.jnatprod.7b00197
8. Peerzada AM, Ali HH, Naeem M, Latif M, Bukhari AH, Tanveer A (2015) *Cyperus rotundus* L.: traditional uses, phytochemistry, and pharmacological activities. J Ethnopharmacol 174:540–560. https://doi.org/10.1016/j.jep.2015.08.012
9. Sunil AG, Kesavanarayanan KS, Kalaivani P, Sathiya S, Ranju V, Priya RJ, Pramila B, Paul FDS, Venkhatesh J, Babu CS (2011) Total oligomeric flavonoids of *Cyperus rotundus* ameliorates neurological deficits, excitotoxicity and behavioral alterations induced by cerebral ischemic–reperfusion injury in rats. Brain Res Bull 84:394–405. https://doi.org/10.1016/j.brainresbull.2011.01.008
10. Hemanth Kumar K, Tamatam A, Pal A, Khanum F (2013) Neuroprotective effects of *Cyperus rotundus* on SIN-1 induced nitric oxide generation and protein nitration: ameliorative effect against apoptosis mediated neuronal cell damage. NeuroToxicology 34:150–159. https://doi.org/10.1016/j.neuro.2012.11.002
11. Sukjamnong S, Santiyanont R (2012) Antioxidant activity of *Fimbristylis ovata* and its effect on RAGE gene expression in human lung adenocarcinoma epithelial cell line. J Chem Pharm Res 4:2483–2489. ISSN: 0975-7384
12. Sukjamnong S, Santiyanont R (2015) Effect of *Fimbristylis ovata* on receptor for advanced glycation end-products, proinflammatory cytokines, and cell adhesion molecule level and gene expression in U937 and bEnd.3 cell lines. Genet Mol Res 14:3984–3994. https://doi.org/10.4238/2015.April.27.13
13. Thomas S, Priya EJS (2015) Effect of *Fimbristylis ovata* (Burm. F) J. Kern on vero cell and MCF-7 cell morphology. J Chem Pharm Res 7:284–290. ISSN:0975-7384
14. Soman S, Raju R, Sandhya VK, Advani J, Khan AA, Harsha HC, Prasad TS, Sudhakaran PR, Pandey A, Adishesha PK (2013) A multicellular signal transduction network of AGE/RAGE signaling. J Cell Commun Signal 7:19–23. https://doi.org/10.1007/s12079-012-0181-3
15. Li J, Schmidt AM (1997) Characterization and functional analysis of the promoter of RAGE, the receptor for advanced glycation end products. J Biol Chem 272:16498–16506. https://doi.org/10.1074/jbc.272.26.16498
16. Mattson MP, Camandola S (2001) NF-kappaB in neuronal plasticity and neurodegenerative disorders. J Clin Investig 107:247–254. https://doi.org/10.1172/JCI11916
17. Lanzillotta A, Porrini V, Bellucci A, Benarese M, Branca C, Parrella E, Spano PF, Pizzi M (2015) NF-κB in innate neuroprotection and age-related neurodegenerative diseases. Front Neurol 6:98. https://doi.org/10.3389/fneur.2015.00098
18. Fogal B, Hewett SJ (2008) Interleukin-1beta: a bridge between inflammation and excitotoxicity? J Neurochem 106:1–23. https://doi.org/10.1111/j.1471-4159.2008.05315.x
19. Galic MA, Riazi K, Pittman QJ (2012) Cytokines and brain excitability. Front Neuroendocrinol 33:116–125. https://doi.org/10.1016/j.yfrne.2011.12.002
20. Abraham E (2000) NF-κB activation. Crit Care Med 28:N100–N104. https://doi.org/10.1097/00003246-200004001-00012
21. Tak PP, Firestein GS (2001) NF-κB: a key role in inflammatory diseases. J Clin Investig 107:7–11. https://doi.org/10.1172/JCI11830
22. Fuchs CS, Simon RC, Riethorst W, Zepeck F, Kroutil W (2014) Synthesis of (R)- or (S)-valinol using ω-transaminases in aqueous and organic media. Bioorg Med Chem 22:5558–5562. https://doi.org/10.1016/j.bmc.2014.05.055
23. Chen TT, Jiandong L, Wang G, Jiang SL, Li LB, Gao CQ (2013) Combined treatment of ulinastatin and tranexamic acid provides beneficial effects by inhibiting inflammatory and fibrinolytic response in patients undergoing heart valve replacement surgery. Heart Surg Forum 16:E38–E47. https://doi.org/10.1532/HSF98.20121072
24. Teng Y, Feng C, Liu Y, Jin H, Gao Y, Li T (2018) Anti-inflammatory effect of tranexamic acid against trauma-hemorrhagic shock-induced acute lung injury in rats. Exp Anim 67:313–320. https://doi.org/10.1538/expanim.17-0143
25. Wang B (2009) Sialic acid is an essential nutrient for brain development and cognition. Annu Rev Nutr 29:177–222. https://doi.org/10.1146/annurev.nutr.28.061807.155515
26. Schnaar RL, Gerardy-Schahn R, Hildebrandt H (2014) Sialic acids in the brain: gangliosides and polysialic acid in nervous system development, stability, disease, and regeneration. Physiol Rev 94:461–518. https://doi.org/10.1152/physrev.00033.2013
27. Dewanjee S, Maiti A, Das AK, Mandal SC, Dey SP (2009) Swietenine: a potential oral hypoglycemic from *Swietenia macrophylla* seed. Fitoterapia 80:249–251. https://doi.org/10.1016/j.fitote.2009.02.004
28. Sun YP, Jin WF, Wang YY, Wang G, Morris-Natschke SL, Liu JS, Wang GK, Lee KH (2018) Chemical structures and biological activities of limonoids from the genus *Swietenia* (Meliaceae). Molecules 23. https://doi.org/10.3390/molecules23071588
29. Oliveira LT, Leon GVO, Provance DW Jr, de Mello FG, Sorenson MM, Salerno VP (2015) Exogenous beta-amyloid peptide interferes with GLUT4 localization in neurons. Brain Res 1615:42–50. https://doi.org/10.1016/j.brainres.2015.04.026
30. de Nazareth AM (2017) Type 2 diabetes mellitus in the pathophysiology of Alzheimer's disease. Dement Neuropsychol 11:105–113. https://doi.org/10.1590/1980-57642016dn11-020002
31. Li Y, Chi G, Shen B, Tian Y, Feng H (2016) Isorhamnetin ameliorates LPS-induced inflammatory response through downregulation of NF-κB signaling. Inflammation 39:1291–1301. https://doi.org/10.1007/s10753-016-0361-z
32. Choi YH (2016) The cytoprotective effect of isorhamnetin against oxidative stress is mediated by the upregulation of the

Nrf2-dependent HO-1 expression in C2C12 myoblasts through scavenging reactive oxygen species and ERK inactivation. Gen Physiol Biophys 35:145–154. https://doi.org/10.4149/gpb_2015034

33. Ishola IO, Osele MO, Chijioke MC, Adeyemi OO (2019) Isorhamnetin enhanced cortico-hippocampal learning and memory capability in mice with scopolamine-induced amnesia: role of antioxidant defense, cholinergic and BDNF signaling. Brain Res 1712:188–196. https://doi.org/10.1016/j.brainres.2019.02.017
34. Wang X, Jiao X, Liu Z, Li Y (2017) Crocetin potentiates neurite growth in hippocampal neurons and facilitates functional recovery in rats with spinal cord injury. Neurosci Bull 33:695–702. https://doi.org/10.1007/s12264-017-0157-7
35. Zhang J, Wang Y, Dong X, Liu J (2018) Crocetin attenuates inflammation and amyloid-beta accumulation in APPsw transgenic mice. Immun Ageing 15:24. https://doi.org/10.1186/s12979-018-0132-9
36. Zhu A, Lao C, Wang Z, Chen Y, Bai C (2019) Characterization of crocetin-monoglucuronide as a neuron-protective metabolite of crocin-1. Mol Nutr Food Res e1900024. https://doi.org/10.1002/mnfr.201900024
37. Alison MD, Richard JP, Mark EH, Andrew DA (2003) The synthesis of naturally occurring vitamin K and vitamin K analogues. Curr Org Chem 7:1625–1634. https://doi.org/10.2174/1385272033486279
38. Netscher T (2007) Synthesis of vitamin E, vitamins & hormones. Academic Press, Cambridge, pp 155–202. https://doi.org/10.1016/S0083-6729(07)76007-739
39. Bourre JM (2004) Roles of unsaturated fatty acids (especially omega-3 fatty acids) in the brain at various ages and during ageing. J Nutr Health Aging 8:163–174
40. Mahmoudi R, Ghareghani M, Zibara K, Tajali Ardakani M, Jand Y, Azari H, Nikbakht J, Ghanbari A (2019) Alyssum homolocarpum seed oil (AHSO), containing natural alpha linolenic acid, stearic acid, myristic acid and beta-sitosterol, increases proliferation and differentiation of neural stem cells in vitro. BMC Complement Altern Med 19:113. https://doi.org/10.1186/s12906-019-2518-4
41. Barnham KJ, Masters CL, Bush AI (2004) Neurodegenerative diseases and oxidative stress. Nat Rev Drug Discov 3:205–214. https://doi.org/10.1038/nrd1330
42. Butterfield DA, Halliwell B (2019) Oxidative stress, dysfunctional glucose metabolism and Alzheimer disease. Nat Rev Neurosci 20:148–160. https://doi.org/10.1038/s41583-019-0132-6
43. Heppner FL, Ransohoff RM, Becher B (2015) Immune attack: the role of inflammation in Alzheimer disease. Nat Rev Neurosci 16:358. https://doi.org/10.1038/nrn3880